

Humidity-triggered self-healing films with excellent oxygen barrier performance†

Cite this: *Chem. Commun.*, 2014, 50, 7136

Received 17th March 2014,
Accepted 13th May 2014

DOI: 10.1039/c4cc01970a

www.rsc.org/chemcomm

Yibo Dou, Awu Zhou, Ting Pan, Jingbin Han,* Min Wei,* David G. Evans and
Xue Duan

Hybrid films were fabricated via layer-by-layer assembly of layered double hydroxide (LDH) nanoplatelets and poly(sodium styrene-4-sulfonate) (PSS) followed by subsequent permeation of poly(vinyl alcohol) (PVA), which show excellent oxygen barrier performance with humidity-triggered self-healing capability.

With the extremely high oxygen barrier requirements needed for applications ranging from food packaging to encapsulation of electronic devices and even fuel cells,^{1,2} a variety of hybrid films consisting of polymeric matrices and two-dimensional (2D) inorganic flakes have been designed and fabricated.^{3–5} Although considerable efforts have been devoted to achieve barrier films with low oxygen permeability, high transparency and good flexibility, the construction of gas barrier films with long-term durability still remains a challenging goal. The flexing of these barrier films as well as crack formation during usage allow the influx of oxygen, which would result in the sharp decrease and unrecoverability of the barrier property. This issue is regarded as a serious problem in maintaining long lifetime of gas barrier films for practical applications. Therefore, how to explore new materials or approaches to obtain high barrier films with excellent durability is an urgent problem to be solved.

Self-healing materials possess the capability of repairing themselves under external stimuli (photo illumination, electric, thermal treatment, *etc.*) after damage, which is a striking property that can prolong their lifetime.^{6–8} By virtue of the excellent gas barrier property of 2D inorganic nanoplatelets, designing a hybrid structure constructed by inorganic nanoplatelets and self-healing polymers would be a feasible solution to the aforementioned durability issues in gas barrier materials. This strategy allows us to present the synergistic effect of the components: on the one hand, the highly-oriented nanoplatelets induce a long diffusion length and strong resistance to oxygen, thus suppressing the gas permeability; on the other hand, the self-healing polymer is capable of

autonomic repairing of severe damaged areas, giving rise to longer lifetime of gas barrier films.

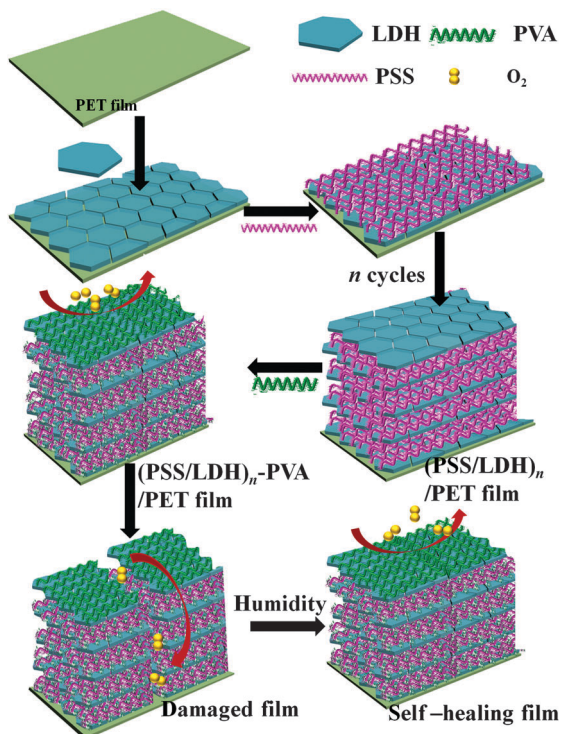
As one type of important 2D inorganic materials, layered double hydroxides (LDHs) have been widely used for the fabrication of organic–inorganic hybrid materials with enhanced mechanical, thermal and photo-functional properties.^{9–11} With regard to self-healing polymers, poly(vinyl alcohol) (PVA) possesses advantages of low cost, easy manufacture and good biocompatibility, whose self-healing ability relies on formation of hydrogen bonds between hydroxyl groups of PVA chains on the crack areas when exposed to moisture.^{12,13} In this work, we reported a self-healing film with high gas barrier performance *via* layer-by-layer (LBL) assembly of poly(sodium styrene-4-sulfonate) (PSS) and LDH nanoplatelets followed by incorporation of PVA (Scheme 1). Owing to the high orientation imparted by LDH nanoplatelets, the (LDH–PSS)_{*n*}–PVA film exhibits largely enhanced oxygen barrier properties. Furthermore, the film is capable of self-repairing the crack areas upon humidity stimulation. This work provides a novel strategy to realize multifunctional films with excellent gas barrier behavior and self-healing ability simultaneously, which is expected to be used in food packaging, electronic device encapsulation and the biomedical field.

The MgAl–LDH nanoplatelets were synthesized according to the separate nucleation and aging steps method reported by our group.¹⁴ The XRD pattern and the FT-IR spectrum (Fig. S1A and B, ESI†) indicating well-defined NO₃–LDH with high crystallization were obtained. The TEM image reveals a narrow size distribution (80–120 nm) of the individual hexagonal LDH nanoplatelets (Fig. S1C, ESI†). A clear Tyndall light scattering was observed (Fig. S1D, ESI†), illustrating a stable and transparent colloidal suspension. The LDH nanoplatelets were then used as building blocks to fabricate (LDH–PSS)_{*n*} films by the LBL assembly method. The UV-vis spectra of the resulting (LDH–PSS)_{*n*} films display a strong absorption band at 193 nm attributed to PSS (Fig. 1), whose intensity increases linearly with the bilayer number *n* (inset of Fig. 1), indicating a stepwise and regular film growth procedure. Moreover, side-view SEM images (Fig. S2A–D, ESI†) illustrate that the thickness of (LDH–PSS)_{*n*} films increases linearly from ~98 nm to ~420 nm when *n* varies from 5 to 20, demonstrating an average thickness of

State Key Laboratory of Chemical Resource Engineering, Beijing University of
Chemical Technology, Beijing 100029, P. R. China.

E-mail: hanjb@mail.buct.edu.cn, weimin@mail.buct.edu.cn; Tel: +86-10-64412131

† Electronic supplementary information (ESI) available: XRD; AFM; TEM; UV-vis spectra; OTR tests. See DOI: 10.1039/c4cc01970a



Scheme 1 Schematic illustration of the fabrication of $(\text{LDH-PSS})_n$ -PVA film on a polyester (PET) substrate serving as oxygen barrier film with self-healing ability.

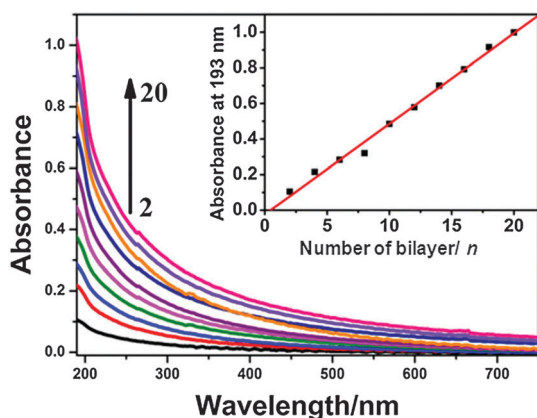


Fig. 1 UV-vis spectra of the $(\text{LDH-PSS})_n$ ($n = 2-20$) films (inset: the linear relationship between absorbance at 193 nm and bilayer number n).

~ 21 nm for one LDH-PSS bilayer (Fig. S3, ESI[†]). In addition, the obtained $(\text{LDH-PSS})_{20}$ -PVA film displays an increased absorption intensity at 193 nm compared with $(\text{LDH-PSS})_{20}$ film (Fig. S4, ESI[†]).

The top-view SEM image of $(\text{LDH-PSS})_{20}$ film displays a homogeneous distribution of LDH nanoplatelets on the film surface, and a rough cross-section with a thickness of ~ 420 nm was observed in the side-view SEM image (Fig. 2A). In contrast, after treatment by PVA, a more smooth, continuous surface and cross-section (Fig. 2B) were observed for the $(\text{LDH-PSS})_{20}$ -PVA film, with a slight increase in film thickness (~ 425 nm). It should be noted that the minimum PVA coating of ~ 5 nm was chosen in this work. A thin PVA coating

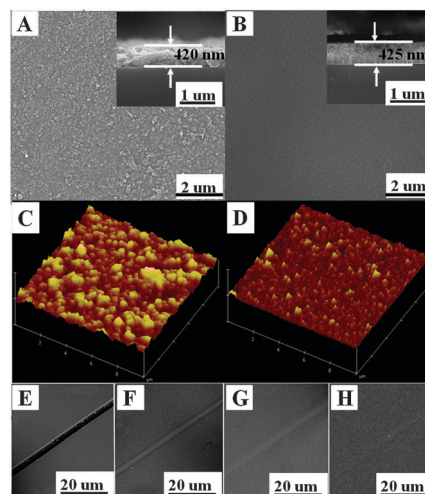


Fig. 2 SEM images of (A) $(\text{LDH-PSS})_{20}$ and (B) $(\text{LDH-PSS})_{20}$ -PVA film, respectively (inset: side-view images). AFM images of (C) $(\text{LDH-PSS})_{20}$ and (D) $(\text{LDH-PSS})_{20}$ -PVA film, respectively. (E-H) The SEM images of damaged $(\text{LDH-PSS})_{20}$ -PVA film after immersion in $\sim 85\%$ relative humidity for 0, 25, 50 and 75 h, respectively.

results in a poor self-healing effect; while a much thicker one leads to a prolonged self-healing time. In addition, the surface roughness decreases from 24.3 to 6.7 nm, as shown in the AFM images (Fig. 2C and D), demonstrating the permeation of PVA molecules into the interspace of $(\text{LDH-PSS})_{20}$ film, which is of crucial importance for the self-healing property.

The XRD pattern (Fig. S5, ESI[†]) of the $(\text{LDH-PSS})_{20}$ -PVA film displays a peak at $2\theta = 11.2^\circ$ attributed to the (003) reflection of the LDH structure. The absence of any nonbasal reflections ($h, l \neq 0$) compared with the LDH powdered sample (Fig. S1A, ESI[†]) indicates a preferred orientation of LDH with the ab plane parallel to the substrate. Furthermore, the well-dispersed and oriented LDH nanoplatelets render the $(\text{LDH-PSS})_{20}$ -PVA-PET film with a remarkable transparency with an average light transmittance of 90% over the visible-light spectrum (400–800 nm; Fig. S6, ESI[†]).

The SEM images in Fig. 2E–H show the self-healing process of the $(\text{LDH-PSS})_{20}$ -PVA-PET film with an artificial cut damage (~ 2.8 μm in width, Fig. 2E) using a scalpel. An obvious self-healing of the cut was observed by treating the damaged film at $\sim 85\%$ relative humidity (Fig. 2F and G), and the whole healing process was complete after ~ 75 h (Fig. 2H). In a control experiment, the $(\text{LDH-PSS})_{20}$ -PET film without PVA failed to heal the damage under the same conditions (Fig. S7, ESI[†]). Therefore, the self-healing capability of $(\text{LDH-PSS})_{20}$ -PVA-PET film is possibly attributed to the filling of PVA into the interspace of $(\text{LDH-PSS})_{20}$ -PET film followed by the formation of the hydrogen-bonding network upon humidity stimulation.

The barrier properties of the pristine polyester (PET), $(\text{LDH-PSS})_n$ -PET and $(\text{LDH-PSS})_{20}$ -PVA-PET films were studied by oxygen transmission rate (OTR) measurements (Fig. 3A). In contrast to the OTR value of $50.28 \text{ cm}^3 \text{ m}^{-2} \text{ day}^{-1} \text{ atm}^{-1}$ for the pristine PET film, the OTR of $(\text{LDH-PSS})_n$ -PET film decreases from 45.22 to as low as $8.71 \text{ cm}^3 \text{ m}^{-2} \text{ day}^{-1} \text{ atm}^{-1}$ upon increasing n from 5 to 20 and thickness from ~ 96 to ~ 420 nm. Moreover, the control samples without LDH nanoplatelets (*e.g.*, $(\text{PDDA-PSS})_{90}$ -PET and PVA-PET

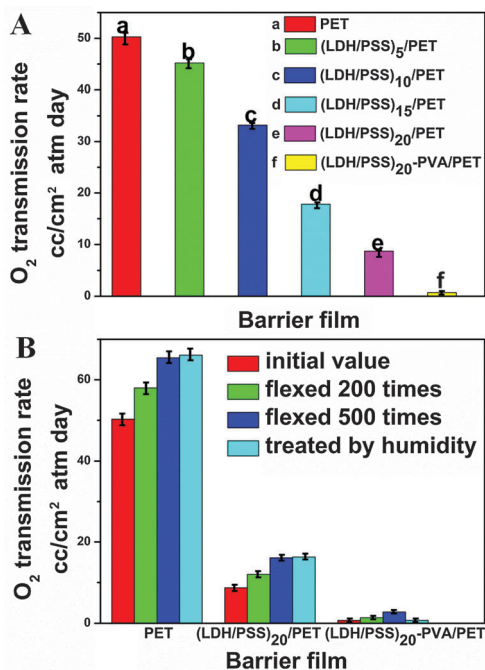


Fig. 3 (A) OTR values for pristine PET, (LDH-PSS)_n-PET ($n = 5, 10, 15, 20$) and (LDH-PSS)₂₀-PVA-PET film, respectively. (B) The variation of OTR values for pristine PET, (LDH-PSS)₂₀-PET and (LDH-PSS)₂₀-PVA-PET film by flexing and humidity treatment, respectively.

film with a thickness of ~ 420 nm) display relatively weak barrier ability (Fig. S8, ESI[†]). The results illustrate that the incorporation of highly-oriented LDH nanoplatelets suppresses the permeability of oxygen, as a result of the increased diffusion length and strong diffusion resistance. After coated with PVA, the OTR decreases sharply to ~ 0.72 cm³ m⁻² day⁻¹ atm⁻¹, which is attributed to the more condensed film with largely enhanced oxygen diffusion resistance. In addition, the oriented film possesses a satisfactory mechanical property (yielding stress = ~ 90 Mpa, strain at break = $\sim 28\%$), which is expected to guarantee its practical application (Fig. S9, ESI[†]).

The long-term durability of the barrier films was further studied by testing the OTR over the samples after hundred times of folding (Fig. 3B). The oxygen barrier capability of all the films was deteriorated upon flexing, indicative of damage formation. However, after being treated by humidity for 75 h (Fig. S10: see self-healing kinetics in the ESI[†]), the (LDH-PSS)₂₀-PVA-PET film recovered its original oxygen barrier property, demonstrating an excellent humidity-triggered self-healing capability. In contrast, both the pure PET and (LDH-PSS)₂₀-PET film do not show self-healing behavior. It is proposed that the hydrogen bond network formed in the (LDH-PSS)₂₀-PVA-PET film with the assistance of water vapor hinders the diffusion of oxygen and maintains the durability of barrier film. In addition, the self-healing capability of (LDH-PSS)₂₀-PVA-PET film can be repeated for several cycles by flexing and humidity treatment alternately (Fig. S11, ESI[†]).

In summary, a humidity-triggered self-healing film was fabricated by LBL assembly of LDH nanoplatelets and PSS followed by incorporation of PVA, which displays excellent oxygen barrier properties and enhanced durability simultaneously. The well-dispersed

and highly-oriented LDH nanoplatelets in the (LDH-PSS)₂₀-PVA-PET film induce a long diffusion length and strong resistance against oxygen, thus suppressing the gas permeability. Most importantly, the obtained film is capable of self-healing crack area by humidity stimulation, owing to the formation of hydrogen-bonding among hydroxyl groups of PVA with the assistance of water molecules. To the best of our knowledge, films with excellent gas barrier behavior and self-healing ability simultaneously have seldom been reported. Therefore, the facile and cost-effective strategy in this work provides a promising approach to address the durability problem in oxygen barrier materials, which has potential applications in the flexible display, druggery and food packaging field.

This work was supported by the 973 Program (Grant No. 2014CB932102), the National Natural Science Foundation of China (NSFC), the Beijing Natural Science Foundation (2132043), the Scientific Fund from Beijing Municipal Commission of Education and the Fundamental Research Funds for the Central Universities (ZD 1303).

Notes and references

- (a) S. Seethamraju, P. Ramamurthy and G. Madras, *RSC Adv.*, 2013, **3**, 12831; (b) J. Gaume, P. Chung, A. Rivaton, S. Thérias and J. Gardette, *RSC Adv.*, 2011, **1**, 1471.
- (a) C. Sanchez, P. Belleville, M. Popall and L. Nicole, *Chem. Soc. Rev.*, 2011, **40**, 696; (b) S. Seethamraju, P. Ramamurthy and G. Madras, *RSC Adv.*, 2014, **4**, 11176.
- (a) Y. Yang, L. Bolling, M. Haile and J. Grunlan, *RSC Adv.*, 2012, **2**, 12355; (b) M. W. Möller, T. Lunkenbein, H. Kalo, M. Schieder, D. A. Kunz and J. Breu, *Adv. Mater.*, 2010, **22**, 5245; (c) C. Aulin, G. Alvarez and T. Lindström, *Nanoscale*, 2012, **4**, 6622.
- O. C. Compton, S. Kim, C. Pierre, J. M. Torkelson and S. T. Nguyen, *Adv. Mater.*, 2010, **22**, 4759.
- T. Ebina and F. Mizukami, *Adv. Mater.*, 2007, **19**, 2450.
- (a) Y. Dou, J. Han, T. Wang, M. Wei, D. G. Evans and X. Duan, *Langmuir*, 2012, **28**, 9535; (b) M. Varnoozfaderani, A. GhavamiNejad, S. Hashmi and F. Stadler, *Chem. Commun.*, 2013, **49**, 4685; (c) Y. Li, S. Chen, M. Wu and J. Sun, *Adv. Mater.*, 2012, **24**, 4578; (d) K. Toohey, N. Sottos, J. Lewis, J. Moore and S. White, *Nat. Mater.*, 2007, **6**, 581.
- (a) T. Wong, S. Kang, S. Tang, E. Smythe, B. Hatton, A. Grinthal and J. Aizenberg, *Nature*, 2011, **477**, 443; (b) D. Shchukin and H. Möwald, *Small*, 2007, **3**, 926; (c) P. Cordier, F. Tournilhac, C. Soulié-Ziakovic and L. Leibler, *Nature*, 2008, **451**, 977; (d) A. Iyer and L. Lyon, *Angew. Chem., Int. Ed.*, 2009, **48**, 4562.
- (a) H. Wang, Y. Xue, J. Ding, L. Feng, X. Wang and T. Lin, *Angew. Chem., Int. Ed.*, 2011, **50**, 11433; (b) S. Basak, J. Nanda and A. Banerjee, *Chem. Commun.*, 2014, **50**, 2356; (c) J. Cui and A. Campo, *Chem. Commun.*, 2012, **48**, 9302.
- (a) J. L. Gunjekar, T. W. Kim, H. N. Kim, I. Y. Kim and S. J. Hwang, *J. Am. Chem. Soc.*, 2011, **133**, 14998; (b) A. Illaik, C. Taviot-Guého, J. Lavis, S. Commereuc, V. Verney and F. Leroux, *Chem. Mater.*, 2008, **20**, 4854; (c) A. W. Myong, M. S. Song, T. W. Kim, I. Y. Kim, J. Y. Ju, Y. S. Lee, S. J. Kim, J. H. Choy and S. J. Hwang, *J. Mater. Chem.*, 2011, **21**, 4286; (d) C. Markland, G. Williams and D. O'Hare, *J. Mater. Chem.*, 2011, **21**, 17896; (e) Z. P. Xu and P. S. Braterman, *J. Phys. Chem. C*, 2007, **111**, 4021.
- (a) F. Leroux and C. Taviot-Guého, *J. Mater. Chem.*, 2005, **15**, 3628; (b) J. W. Bocclair and P. S. Braterman, *Chem. Mater.*, 1999, **11**, 298.
- (a) H. Greenwell, W. Jones, D. Stamires, P. O'Connord and M. Bradyd, *Green Chem.*, 2006, **8**, 1067; (b) J. A. Gursky, S. D. Blough, C. Luna, C. Gomez, A. N. Luevano and E. A. Gardner, *J. Am. Chem. Soc.*, 2006, **128**, 8376; (c) Q. Wang and D. O'Hare, *Chem. Rev.*, 2012, **112**, 4124.
- H. Zhang, H. Xia and Y. Zhao, *ACS Macro Lett.*, 2012, **1**, 1233.
- J. Liu, G. Song, C. He and H. Wang, *Macromol. Rapid Commun.*, 2013, **34**, 1002.
- J. Han, Y. Dou, M. Wei, D. G. Evans and X. Duan, *Angew. Chem., Int. Ed.*, 2010, **49**, 2171.